

ACCEPTED MANUSCRIPT

## On the detailed mechanical response investigation of PHBV/ PCL and PHBV/ PLGA electrospun mats

To cite this article before publication: Burak Bal *et al* 2019 *Mater. Res. Express* in press <https://doi.org/10.1088/2053-1591/ab0eaa>

### Manuscript version: Accepted Manuscript

Accepted Manuscript is “the version of the article accepted for publication including all changes made as a result of the peer review process, and which may also include the addition to the article by IOP Publishing of a header, an article ID, a cover sheet and/or an ‘Accepted Manuscript’ watermark, but excluding any other editing, typesetting or other changes made by IOP Publishing and/or its licensors”

This Accepted Manuscript is © 2019 IOP Publishing Ltd.

During the embargo period (the 12 month period from the publication of the Version of Record of this article), the Accepted Manuscript is fully protected by copyright and cannot be reused or reposted elsewhere.

As the Version of Record of this article is going to be / has been published on a subscription basis, this Accepted Manuscript is available for reuse under a CC BY-NC-ND 3.0 licence after the 12 month embargo period.

After the embargo period, everyone is permitted to use copy and redistribute this article for non-commercial purposes only, provided that they adhere to all the terms of the licence <https://creativecommons.org/licenses/by-nc-nd/3.0>

Although reasonable endeavours have been taken to obtain all necessary permissions from third parties to include their copyrighted content within this article, their full citation and copyright line may not be present in this Accepted Manuscript version. Before using any content from this article, please refer to the Version of Record on IOPscience once published for full citation and copyright details, as permissions will likely be required. All third party content is fully copyright protected, unless specifically stated otherwise in the figure caption in the Version of Record.

View the [article online](#) for updates and enhancements.

## On the Detailed Mechanical Response Investigation of PHBV/ PCL and PHBV/ PLGA Electrospun Mats

Burak Bal<sup>1</sup>, Ibrahim Burkay Tugluca<sup>1</sup>, Nuray Koc<sup>2</sup>, Ismail Alper Isoglu<sup>2,\*</sup>

<sup>1</sup> Department of Mechanical Engineering, Abdullah Gül University, 38080 Kayseri, Turkey

<sup>2</sup> Department of Bioengineering, Abdullah Gül University, 38080 Kayseri, Turkey

### Abstract

In this study, electrospun mats of pristine poly( $\epsilon$ -caprolactone) (PCL), Poly(D,L-lactide-co-glycolide) (PLGA), poly(3-hydroxybutyrate-co-3-hydroxyvalerate) (PHBV), as well as PHBV/PCL blends and PHBV/PLGA blends in different ratios (80:20, 75:25, 50:50, 25:75, 20:80, 10:90, 5:95%, w/w) and Centella Asiatica (CA) loaded (1, 5, 10%, w/v) PHBV/PCL and PHBV/PLGA polyester blends were prepared. Electrospun mats were characterized by scanning electron microscopy (SEM) in order to show uniform and bead and defect-free fiber structure with average diameter. The blend ratio and strain rate dependencies of mechanical behavior of these electrospun membranes were investigated under tensile loading. The tensile tests were conducted at an initial strain rates of  $10^{-1} \text{ s}^{-1}$ ,  $10^{-2} \text{ s}^{-1}$ ,  $10^{-3} \text{ s}^{-1}$  and  $10^{-4} \text{ s}^{-1}$  at room temperature and the best and worst combinations of PHBV/PLGA, PHBV/PCL blend ratios for both stress and ductility required applications were specified for each strain rate. The effects of blend ratios on the tensile strength and Young's modulus were also investigated. Moreover, the effects of Centella Asiatica on the electrospun membranes' mechanical behavior were demonstrated at different strain rates. Consequently, this study constitutes an important guideline for the selection and usage of the aforementioned electrospun membranes as a wound dressing material in terms of mechanical response at different loading scenarios.

*Keywords: Mechanical response, tension test, strain rate, electrospinning, membranes.*

---

\*Corresponding author. [alper.isoglu@agu.edu.tr](mailto:alper.isoglu@agu.edu.tr). Abdullah Gul University Sumer Campus, 38080 Kocasinan/Kayseri, Turkey.

## 1. Introduction

Wound treatment is a one of the major healthcare problems, which affects millions of people worldwide [1]. The wound healing is a very complex and interactive process that combines the multiple cell types including dermal and epidermal cells, immune cells, extracellular matrix (ECM), plasma-derived proteins and growth factors in the regeneration of the skin tissue [1–3]. Besides conventional wound care materials possessing multiple drawbacks such as poor longevity, durability, strength, and enzymatic resistance, skin substitutes prepared from both bioactive natural and synthetic polymers are good candidates for wound dressing materials due to their unique properties including enzymatic degradation resistance, ability to support cell growth, excellent biocompatibility, strength/durability and controlled degradation [4].

A broad range of wound dressing materials have been prepared by using different methods including self-assembly, phase separation, wet spinning and electrospinning [5]. Electrospinning is a fabrication technique in order to obtain fine fibers with a diameter from nano- to micrometer scale by applying high voltage between the solution and the collecting target [6]. In last two decades, it has gained great interest globally due to its flexibility, cost effectiveness, ease of use, ability to align structures, and control the diameters of the fibers [7–9]. Compared to the conventional wound dressing products, electrospun materials possess exceptional features including well biomimicking of the ECM, improved promotion of hemostasis, permeability, conformability to the wound and avoidance of scar induction. Moreover, high surface area to volume of the electrospun materials allows better cell attachment and prevents fluid accumulation to the wounds. A broad variety of different natural and synthetic polymers solved in a proper solvent can be used for obtaining electrospun membranes for biomedical applications including wound dressing, regenerative

1  
2  
3 medicine, tissue engineering and drug delivery systems [5,10–13].  
4  
5

6 Poly( $\epsilon$ -caprolactone) (PCL), poly( $\alpha$ -hydroxy acids) based on lactic and glycolic acid  
7 monomers and their copolymers are the most widely used among all synthetic polymers in the  
8 electrospinning technique. Polyhydroxyalkanoates (PHAs) obtained by biosynthetic pathways  
9 are also preferred for preparing electrospun mats. PCL, semi-crystalline polyester, is one of  
10 the most promising biodegradable polymers used in electrospinning applications due to its  
11 mechanical and structural properties [14]. Particularly, nanofibrous membranes obtained by  
12 the electrospun PCL fibers have elastic morphology with highly interconnected pore structure,  
13 which allows gas exchange and adsorption of exudate and its elasticity and makes the  
14 dressing flexible with the movement of the body parts in wound care application [15]. Despite  
15 the many benefits, electrospun PCL scaffolds have some drawbacks affecting the wound  
16 healing process. Especially, due to porous surface structure, electrospun PCL mats tend to  
17 adhere strongly to wound, which can cause damage on the repaired skin tissue and extend the  
18 time of the healing process, when they are taken out from the wounded area [15]. In addition,  
19 similar to the other aliphatic polyesters, the high hydrophobicity of PCL hinders its  
20 widespread use as a wound dressing substrate [16]. Poly(D,L-lactide-co-glycolide) (PLGA) is  
21 a FDA-approved biodegradable copolymer of poly(lactic acid) (PLA) and poly(glycolic acid)  
22 (PLG). Based on the degree of polymerization and the ratio of the two monomers, PLGA has  
23 tunable degradation and unique mechanical properties, which make them a good candidate for  
24 the wound dressing applications [3]. Polyhydroxyalkanoates (PHAs) are biodegradable  
25 polyesters produced by microorganisms and have been used as biomaterials due to its  
26 biocompatibility [17]. Only several PHAs including poly 3-hydroxybutyrate (PHB), poly(3-  
27 hydroxybutyrate-co-3-hydroxyvalerate) (PHBV), poly 4-hydroxybutyrate (P4HB),  
28 copolymers of 3-hydroxybutyrate and 3-hydroxyhexanoate (PHBHHx) and poly 3-  
29 hydroxyoctanoate (PHO) have been actively investigated in biomedical applications so far  
30  
31  
32  
33  
34  
35  
36  
37  
38  
39  
40  
41  
42  
43  
44  
45  
46  
47  
48  
49  
50  
51  
52  
53  
54  
55  
56  
57  
58  
59  
60

1  
2  
3 [18]. It was also reported that arranging the ratio of the PHA compositions allows controlling  
4 the rate of biocompatibility, the level of mechanical properties and the degradation time under  
5 the certain physical circumstances [19].  
6  
7  
8

9  
10 The recent studies reveal that the wound dressing materials prepared by electrospun polymer  
11 blends of synthetic and natural polymers demonstrate synergetic effect and desirable  
12 advantages on wound healing process, which cannot be achieved by individual polymers [16].  
13 Shi et al. prepared electrospun quaternary ammonium salts-functionalized PCL-gelatin hybrid  
14 membrane for a novel wound dressing possessing long-acting antibacterial properties [20]. In  
15 another study, Tra Thanh et al. fabricated plasma treated electrospun PCL scaffold coated  
16 with silver nanoparticles (AgNPs) embedded in gelatin to enhance its antibacterial property  
17 and minimize the adhesion of scaffold on the wound area [15]. In 2018, Liao et al. developed  
18 a hybrid alginate hydrogel crosslinked by calcium gluconate crystals deposited in PCL-b-  
19 PEG-b-PCL porous microspheres for wound healing [21]. Ehterami et al. prepared  
20 electrospun PCL/collagen nanofibrous matrices loaded with insulin delivering chitosan  
21 nanoparticles as a potential wound healing material [16]. Chanda et al. provided a bilayered  
22 polymeric scaffold obtained by electrospinning method using chitosan/PCL and hyaluronic  
23 acid as a new wound dressing [6]. In another study conducted by Paskiabi et al., an  
24 electrospun PCL/gelatin fibers containing terbinafine hydrochloride for as an antifungal  
25 wound dressing were provided [22]. Abdalkarim et al. prepared electrospun PHBV/cellulose  
26 reinforced nanofibrous membranes with ZnO nanocrystals for wound healing [23]. In 2015,  
27 Lei et al. prepared PHBV/silk fibroin nanofibrous scaffolds for repairing of skin tissue [24].  
28 Varshosaz et al. investigated electrospun poly(methyl vinyl ether-co-maleic acid)/poly(lactic-  
29 co-glycolic acid) nanofibers loaded with montelukast as a new wound care material [25]. In  
30 another study, Liu et al. provided ciprofloxacin-loaded PLGA/sodium alginate electrospun  
31 mats for wound healing [26]. Furthermore, Tohidi et al. proposed a PLGA/chitosan  
32  
33  
34  
35  
36  
37  
38  
39  
40  
41  
42  
43  
44  
45  
46  
47  
48  
49  
50  
51  
52  
53  
54  
55  
56  
57  
58  
59  
60

1  
2  
3 electrospun membrane with amoxicillin-loaded halloysite nanoclay [27]. Daranarong et al.  
4 prepared electrospun fibrous scaffolds of polyhydroxybutyrate (PHB) with various loadings  
5 of poly(L-lactide-co- $\epsilon$ -caprolactone) (PLCL) for nerve tissue engineering. They showed that  
6 PLCL/PHB blend scaffolds have reduced tensile strength and better adhesion and  
7 proliferation performance of olfactory ensheathing cells (OECs) compare to neat PLCL  
8 electrospun scaffolds [28]. In other study, Ding et al. fabricated fibrous mats of  
9 PHB/PCL/58S blends using electrospinning and sol-gel methods and investigated the cell  
10 adhesion, viability, proliferation and ALP activity of MG-63 osteoblast-like cells on the  
11 scaffolds [29]. Ublekov et al. provided electrospun poly( $\beta$ -hydroxybutyrate) (PHB) and  
12 poly(3-hydroxybutyrate-co-3-hydroxyvalerate) (PHBV)/organo-modified montmorillonite  
13 (OMMT) nanocomposite fibrous scaffolds and reported the mechanical properties of the  
14 hybrid scaffolds [30].

15  
16  
17 All of these studies in the literature mentioned above, the researchers mainly focused on the  
18 morphology, wettability, water absorption capacity, drug release behavior, and cytotoxic and  
19 antibacterial activity of the electrospun materials. However, in spite of many works on these  
20 topics, there are only a limited number of studies focusing on the mechanical properties of the  
21 membranes. Although, electrospun nanofibrous membranes have many advantages, its  
22 mechanical properties are also very important in order to use them as an appropriate wound  
23 dressing material. Especially, the structural integrity and deformability of the nanofibers have  
24 tremendous effect on vitro cell migration, proliferation, differentiation and as well as the cell  
25 morphology and new tissue formation [31]. According to the study published by Baji et al.,  
26 one of the main problems faced in this field is to determine the tensile behavior of the  
27 nanofibers. Very few studies in the literature focus on the explanation of the phenomenon  
28 behind the mechanical integrity of fiber network structures and the characterization of the  
29 mechanical deformation characteristics of the fibers by observing the stress–strain behavior of  
30  
31  
32  
33  
34  
35  
36  
37  
38  
39  
40  
41  
42  
43  
44  
45  
46  
47  
48  
49  
50  
51  
52  
53  
54  
55  
56  
57  
58  
59  
60

1  
2  
3 the electrospun membranes [32]. However, to the best of the author's knowledge the detailed  
4 mechanical behavior of the electrospun membranes at different blend ratios and strain rates  
5 has never been conducted yet.  
6  
7  
8  
9

10 In this study, we aimed to focus on determining the effects of chemical composition, strain  
11 rate, and a traditional medicinal plant widely known for its wound healing ability, namely  
12 Centella Asiatica (CA), on the mechanical responses of the electrospun PHBV/PCL and  
13 PHBV/PLGA blend membranes. Specifically, all the tensile tests were conducted at 4  
14 different strain rates and several blend ratios and the corresponding engineering stress-strain  
15 behaviors were investigated.  
16  
17  
18  
19  
20  
21  
22  
23  
24

## 25 **2. Materials and methods**

### 26 **2.1 Materials**

27  
28  
29 Poly( $\epsilon$ -caprolactone) (PCL, average  $M_n=80,000$ ; CAS No. 24980-41-4) and poly(3-  
30 hydroxybutyrate-co-3-hydroxyvalerate) (PHBV, natural origin, PHV content 12 mol%,  $M_n=$   
31 280,000,  $M_w=690,000$ ; CAS No.80181-31-3) were supplied by Sigma-Aldrich (USA).  
32  
33 Poly(D,L-lactide-co-glycolide) (PLGA, DL-Lactide:Glycolide copolymer, ratio M/M%:  
34 75/25,  $M_w=120,000$ ; CAS No.26780-50-7) was purchased from Purac Biomaterials (The  
35 Netherlands). Centella Asiatica (CA, natural extract in powder form, CAS No.16830-15-2)  
36 was obtained from Wuhan Yuancheng Technology Development Co. Ltd. (China).  
37  
38 1,1,1,3,3,3-Hexafluoro-2-propanol (HFIP) (CAS No.920-66-1) was purchased from Merck  
39 (USA). All other reagents and solvents are of analytical grade and used without further  
40 purification.  
41  
42  
43  
44  
45  
46  
47  
48  
49  
50  
51  
52  
53

### 54 **2.2 Preparation of electrospun nonwoven mats**

1  
2  
3 PCL, PLGA, PHBV, PHBV/PCL and PHBV/PLGA blends in different ratios (80:20, 75:25,  
4  
5 50:50, 25:75, 20:80, 10:90, 5:95%, w/w) were dissolved in HFIP to prepare the solutions at  
6  
7 the concentration of 20% (w/v) for electrospinning process. CA was added to the PHBV/PCL  
8  
9 (50:50) and PHBV/PLGA (75:25) blend solution at different concentrations (1, 5 and 10%  
10  
11 w/v) and stirred 3h at room temperature in order to obtain homogenous solution. Each  
12  
13 polymer solution was loaded into a 10 mL syringe with 21G needle (with an inner diameter of  
14  
15 14.53 mm) and placed on a motorized and programmable syringe pump (NE-1000 Syringe  
16  
17 Pump, USA). A high voltage power supply (Inovenso NE100, İstanbul, Turkey) was used to  
18  
19 provide the necessary electric potential between the tip and the grounded collector covered  
20  
21 with aluminum foil. The flow rate was set at 1 mL/h and the voltage were applied in the range  
22  
23 of 12-20 kV. The distance between the tip and grounded collector was fixed at 15 cm.  
24  
25  
26  
27  
28  
29  
30  
31

### 32 **2.3 Mechanical testing**

33  
34 After the preparation of the membranes, all of the tensile test specimens were cut according to  
35  
36 the pre-determined dimensions. All of the specimens used for tensile testing were cut into  
37  
38 same dimensions to avoid any possible size effect on the mechanical response of membranes.  
39  
40 The sample specimens were 60 mm in length with 19 mm gauge length, 20 mm in width and  
41  
42 have a thickness of 0.1 mm. Specimens were kept at the room temperature after material  
43  
44 preparation until the tensile tests. Shimadzu AGS-X 10 kN tensile test machine was used for  
45  
46 the tensile tests. Tensile tests were conducted at the strain rates of  $10^{-1} \text{ s}^{-1}$ ,  $10^{-2} \text{ s}^{-1}$ ,  $10^{-3} \text{ s}^{-1}$  and  
47  
48  $10^{-4} \text{ s}^{-1}$  at room temperature. Each of these strain rates was chosen on purpose of observing  
49  
50 the mechanical response of each membrane under possible real-world scenarios.  
51  
52  
53  
54  
55

### 56 **2.4 Materials characterization**

All electrospun nonwoven mats were investigated by using SEM (Carl Zeiss EVO LS10, Germany) after coating with a thin gold layer under vacuum by using sputter coater (Quorum Q150RES, United Kingdom). Fiber diameters were measured from SEM images by using JMicroVision 1.2.7 (National Institutes of Health, Bethesda, MD).

### 3. Results and Discussion

#### 3.2. Fiber structure and morphology

Electrospun nonwoven mats were characterized by SEM to show the bead and defect free morphology of fibers with average diameter, interconnected pores structures and to investigate CA/fibers compatibility. All the fibers were cylindrical, continuous and defect free so it is obvious that the electrospinning process was carried out successfully. Figure 1 and 2 were prepared as representative SEM micrographs of selected membranes. Figure 1a and Figure 1b demonstrate the SEM micrographs of the electrospun PHBV/PLGA (25:75) and CA containing (5%) PHBV/PLGA (25:75) membranes, respectively and they both show uniform fiber diameter distribution without any beads. From Figure 1, it is clearly seen that adding CA decreased the fiber diameter and this trend coincides well with the previous studies in the literature [33]. All the electrospinning parameters were identical (Voltage: 20 kV, flow rate: 1 ml/h, solvent: HFIP, and the distance between the tip and the collector: 15 cm) for both membranes and this decrease in average fiber diameter can be attributed to the fact that adding CA acts as a barrier to the formation of thicker fibers by preventing them to stick the fibers each other. Similar results were also observed previously [34]. The average fiber diameter of the electrospun PHBV/PLGA (25:75) membrane was 1.11  $\mu\text{m}$  (Figure 1a) and PHBV/PLGA (25:75) membrane with CA was 0.67  $\mu\text{m}$  (Figure 1b). These average fiber diameters of the membranes were determined by examining the cross-sections taken from different areas of each sample.

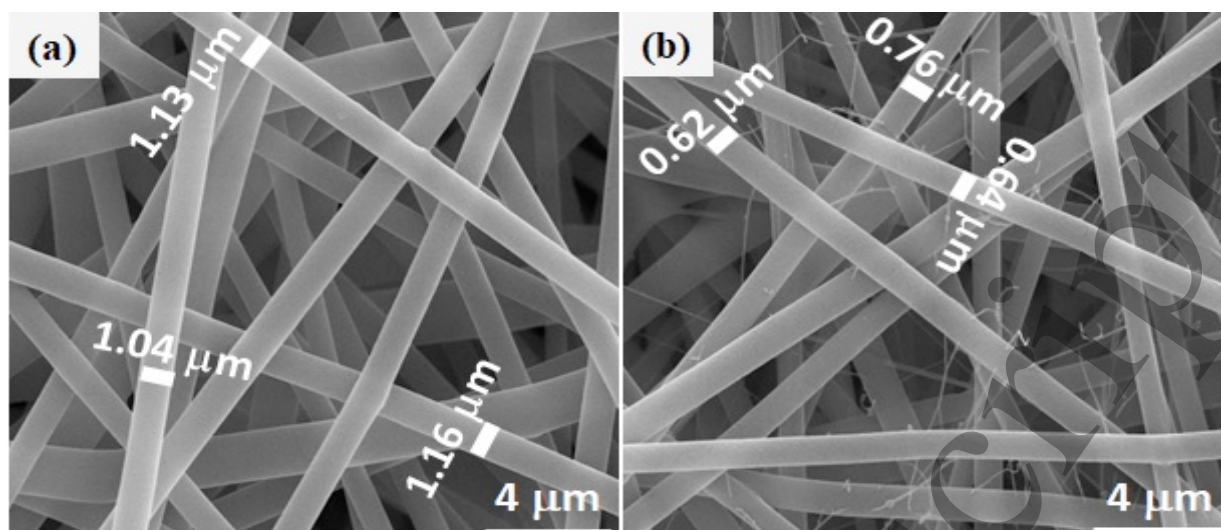


**Figure 1:** SEM images of (a) PHBV/PLGA (25:75) (b) CA containing (5%) PHBV/PLGA (25:75) at 10.0K magnification taken prior to the tensile tests.

Figure 2 a-d show the SEM micrographs of the PHBV/PCL (50:50) membranes without and with addition of CA at different concentrations. Electrospinning conditions (Voltage: 10 kV, flow rate: 1 ml/h, solvent: HFIP and the distance between the tip and the collector: 15 cm) were same for all membranes. The fibers were continuous without any defect. The average fiber diameter of the electrospun PHBV/PCL (50:50) membrane with 0% CA (Figure 2a), 1% CA (Figure 2b), 5% CA (Figure 2c) and 10% CA (Figure 2d) were 1.69 μm, 0.79 μm, 0.69 μm, 0.38 μm, respectively. Therefore, it can easily be seen that increasing the CA concentration decreases the average fiber radius. The decrease in average fiber diameter with the addition of CA is result from the same barrier effect that was explained in the previous paragraph.

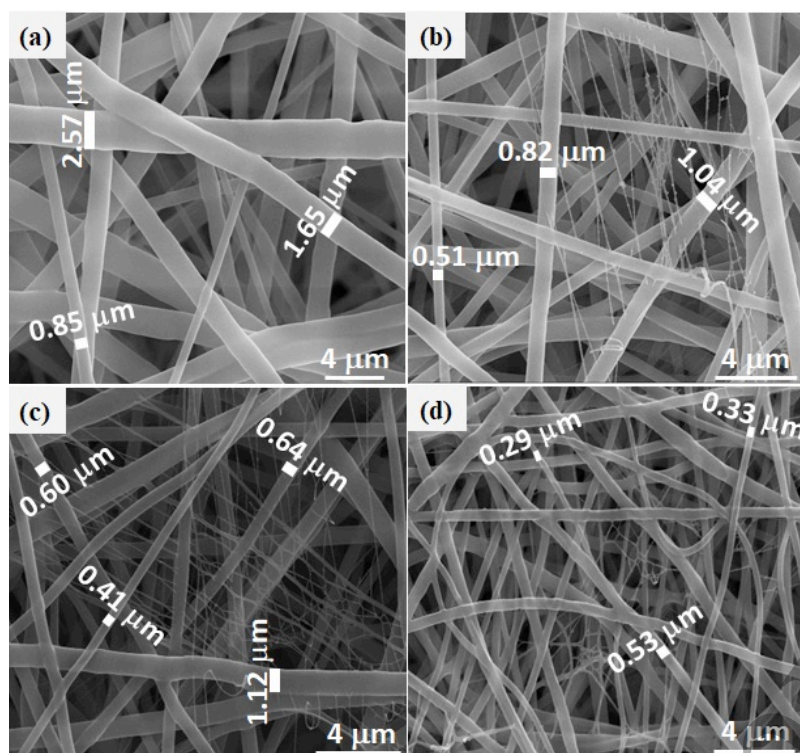


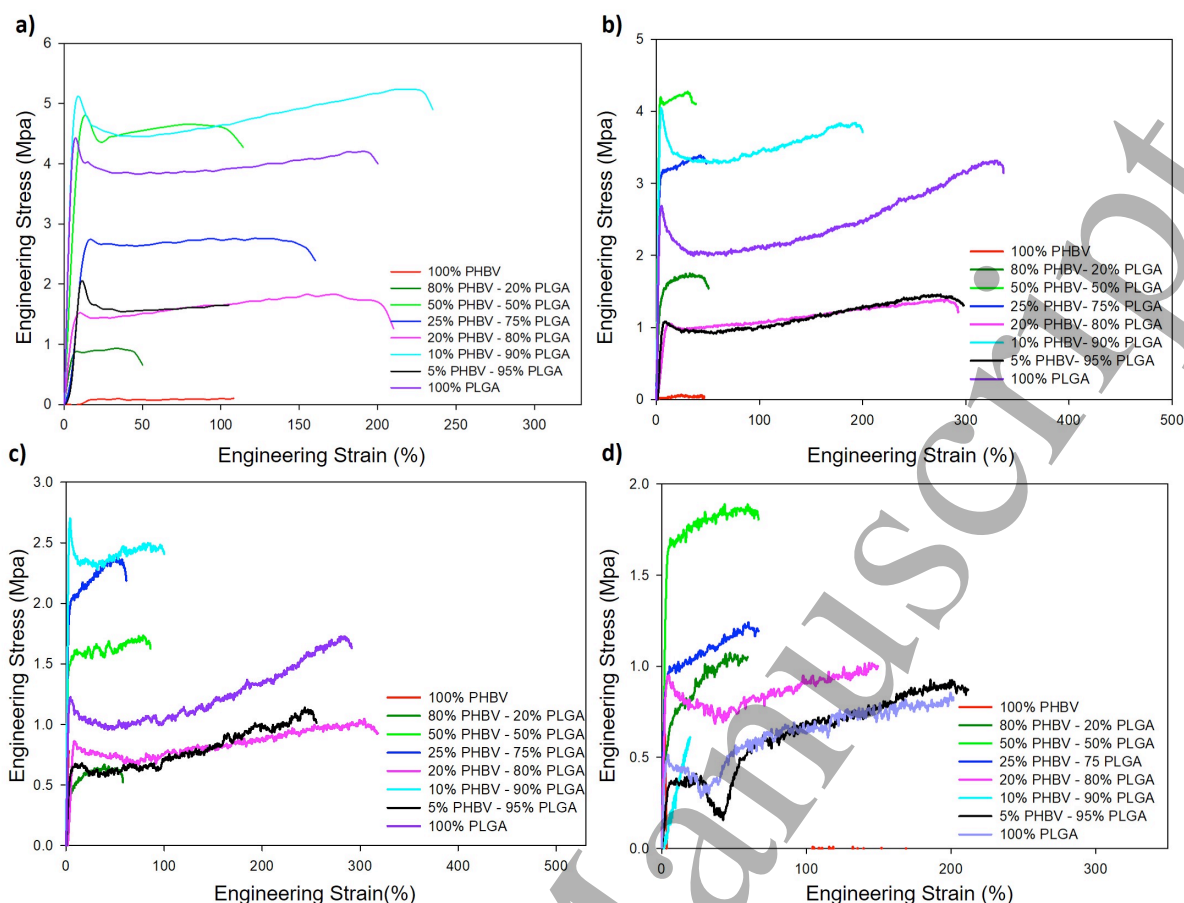
**Figure 2:** SEM of electrospun PHBV/PCL (50:50) (a) 0% CA (b) 1% CA (c) 5% CA (d) 10% CA composite membranes at x 10K magnification taken before tensile tests in their bulk form.

### 3.2. Mechanical behavior

Figure 3 a-d show the blend ratio dependence of the mechanical response of electrospun PHBV/PLGA membranes under tensile loading. Figure 3a shows the engineering stress-strain curves at an initial strain rate of  $1 \times 10^{-1} \text{ s}^{-1}$ . Deformation responses after the major tear were not reported in any of the figures since the membranes lose their usability after a major tear. A significant amount of plastic deformation and necking were observed in almost all the specimens except PHBV/PLGA (80:20) membrane. This observation is common in these kind of polymers in the literature [31,35]. In addition, a noticeable decrease in the flow stress was observed after the yield stress in all the membranes. Consequently, the stress required for yield initiation is greater than the stress required to maintain the plastic flow (yield propagation) and this phenomenon was discussed well in the literature [36]. It was observed that as the PLGA blend ratio increased from 20% to until 90%, ductility of the membranes

1  
2  
3 also increased (Figure 3a). However, further increase in PLGA blend ratio (from 90% to 95%)  
4 decreased the ductility of the membrane around 52%. On the other hand, increasing the PLGA  
5 blend ratio from 95% to 100% doubled the ductility again. In addition, strength of  
6 PHBV/PLGA membranes changed with blend ratios. Specifically, at the strain rate of  $1 \times 10^{-1}$   
7  $s^{-1}$  and room temperature, PHBV/PLGA (10:90) showed the best strength and ductility  
8 combination with the values of 5.2 MPa and 238%, respectively. On the other hand,  
9 PHBV/PLGA (80:20) and PHBV (100) showed the lowest ductility and strength values,  
10 respectively, among all membranes. Figure 3b shows the engineering stress-strain curves at an  
11 initial strain rate of  $1 \times 10^{-2} s^{-1}$ . From this subfigure, it is evident that increasing PLGA  
12 content up to 75% did not change the ductility compared to PLGA-free case considerably, but  
13 enhanced the strength of the membranes. On the contrary, further increase in PLGA content  
14 increased the ductility dramatically. The membrane made of PLGA (100) can be used in  
15 application where high elongation is desired and PHBV/PLGA (10:90) exhibited good  
16 combination of high strength and significant ductility at  $1 \times 10^{-2} s^{-1}$  strain rate. Moreover, if  
17 the membranes are not exposed a stress values greater than 1.6 MPa in application areas,  
18 PHBV/PLGA (80:20) membrane can be used over greater PLGA blend ratios in order to  
19 decrease the cost concerning only mechanical properties. Figure 3c shows the engineering  
20 stress-strain curves at an initial strain rate of  $1 \times 10^{-3} s^{-1}$ . Similar to the previous case,  
21 increasing PLGA concentration until 75% did not affect the ductility considerably.  
22 Interestingly, 80% PLGA increased the ductility prominently, but increasing PLGA  
23 concentration to 90% enhanced the strength dramatically. This increase in strength could not  
24 be accommodated plastically and sudden fracture occurred. This behavior is very common in  
25 steels. In order to increase the strength of steels without sacrificing from ductility can be  
26 attained by adding carbon atom to the material but after critical concentration of carbon in the  
27 chemical concentration ductility decreases and sudden fracture takes place [37]. At this strain  
28  
29  
30  
31  
32  
33  
34  
35  
36  
37  
38  
39  
40  
41  
42  
43  
44  
45  
46  
47  
48  
49  
50  
51  
52  
53  
54  
55  
56  
57  
58  
59  
60

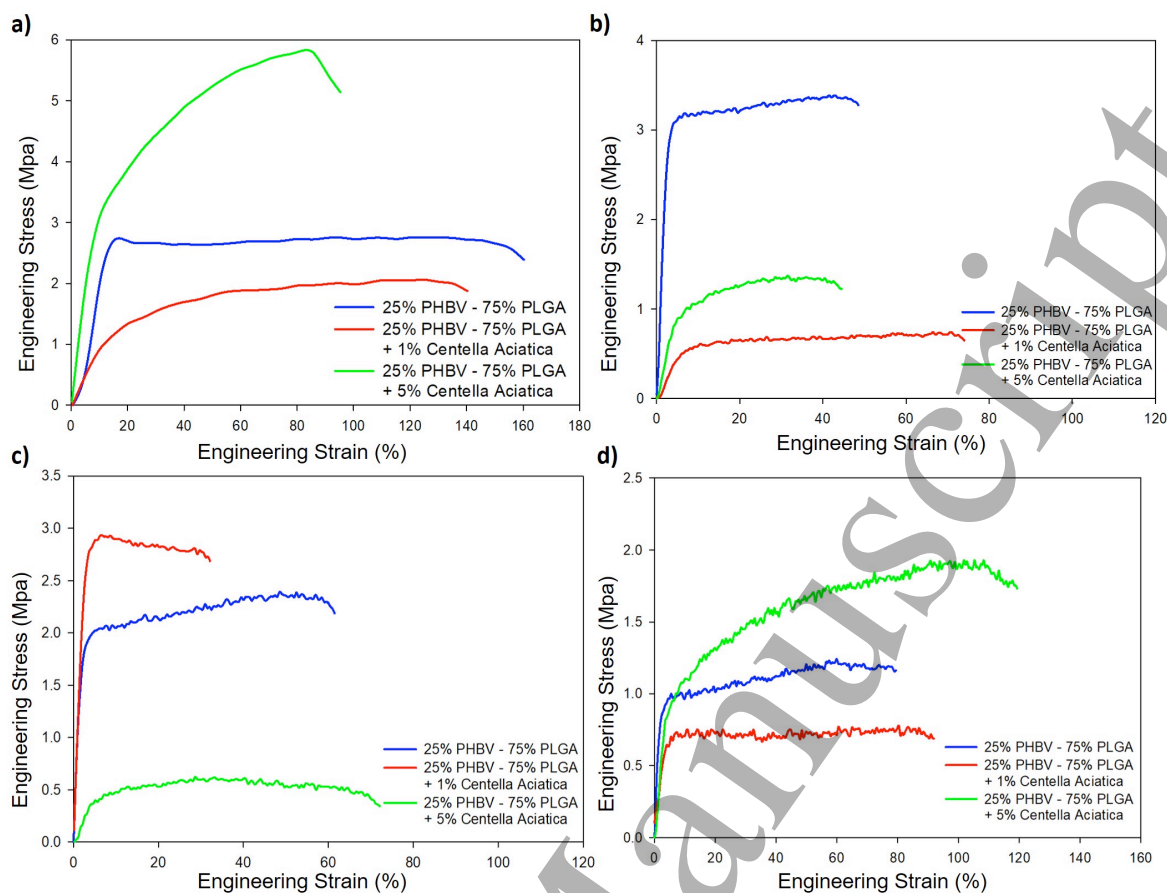
1  
2  
3 rate, in the applications, which require strength but not ductility both, PHBV/PLGA (90:10)  
4 and PHBV/PLGA (25:75) membranes could be good candidates over other electrospun  
5 PHBV/PLGA membranes. However, if the ductility with mid-strength values desired both,  
6 PHBV/PLGA (5:95) and PHBV/PLGA (20:80) membranes can be utilized. Furthermore,  
7 100% PLGA showed great combination of strength and ductility at  $1 \times 10^{-3} \text{ s}^{-1}$  strain rate.  
8 Figure 3d shows the engineering stress-strain curves at an initial strain rate of  $1 \times 10^{-4} \text{ s}^{-1}$ . At  
9 the lowest strain rate, PHBV/PLGA (50:50) showed the greatest strength values compared to  
10 other membranes. Similar to higher strain rate cases, increase in the ductility started after 75%  
11 PLGA ratio. The greatest stress values with more than 100% ductility were attained in  
12 PHBV/PLGA (20:80) membrane. Therefore, at the strain rate of  $1 \times 10^{-4} \text{ s}^{-1}$  PHBV/PLGA  
13 (50:50) membrane can be used in applications, which require high strength without promising  
14 ductility and PHBV/PLGA (20:80) membrane can be used in applications, that require  
15 significant ductility but do not be subjected to high stress values. The current results, which  
16 demonstrate the mechanical responses of PHBV/PLGA blends at different blend ratios and at  
17 different strain rates, are first in the literature.  
18  
19  
20  
21  
22  
23  
24  
25  
26  
27  
28  
29  
30  
31  
32  
33  
34  
35  
36  
37  
38  
39  
40  
41  
42  
43  
44  
45  
46  
47  
48  
49  
50  
51  
52  
53  
54  
55  
56  
57  
58  
59  
60



**Figure 3:** Engineering tensile stress-strain behavior of electrospun PHBV/PLGA membranes with different blend ratios a)  $1 \times 10^{-1} \text{ s}^{-1}$ , b)  $1 \times 10^{-2} \text{ s}^{-1}$ , c)  $1 \times 10^{-3} \text{ s}^{-1}$ , d)  $1 \times 10^{-4} \text{ s}^{-1}$ .

Figure 4 a-d show the effects of CA on the mechanical response of electrospun PHBV/PLGA (25:75) membrane at different strain rates. It can be seen from all the subfigures that adding CA to the chemical composition of PHBV/PLGA membrane changed the mechanical response, considerably. Figure 4a shows the engineering stress-engineering strain curves of the CA-added and CA-free PHBV/PLGA (25:75) membrane at an initial strain rate of  $1 \times 10^{-1} \text{ s}^{-1}$ . Electrospun blend without CA showed the greatest ductility relative to others. Blend with 1% CA in the chemical composition exhibited slightly lower strength values and ductility compared to CA-free membrane. On the other hand, when the CA concentration was increased up to 5%, the strength of the membrane doubled but it also deteriorated the elongation at failure almost 45%. Figure 4b shows the engineering stress-engineering strain

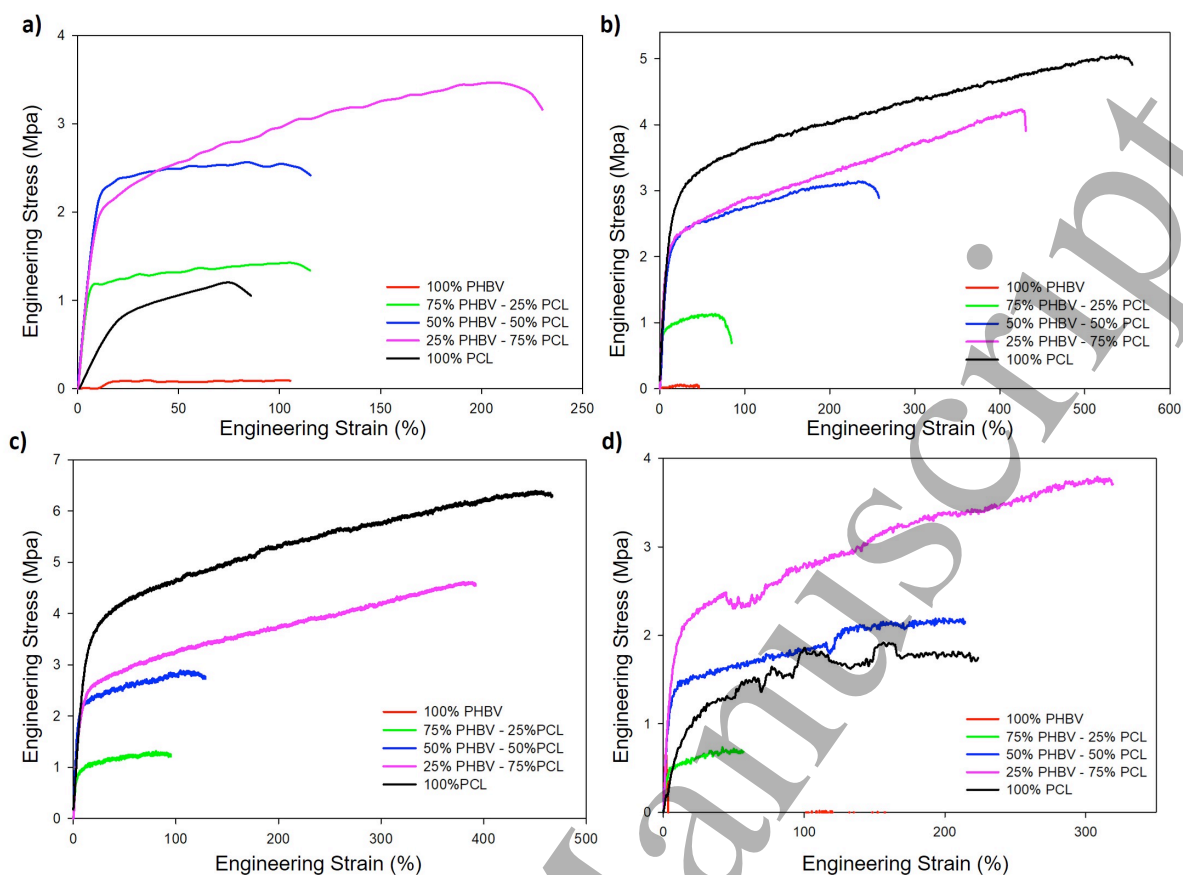
1  
2  
3 curves of the CA-added and CA-free PHBV/PLGA (25:75) membrane at an initial strain rate  
4 of  $1 \times 10^{-2} \text{ s}^{-1}$ . Decreasing strain rate only one order of magnitude resulted dramatic decrease  
5 in the strength values and ductility of both CA-added specimens. Specifically, the tensile  
6 strength and ductility of 5% CA-added membrane were decreased by 45% and 80%,  
7 respectively. At this strain rate, adding CA decreased the strength values at all strains,  
8 however, it had no considerable negative effects on ductility. Figure 4c shows the engineering  
9 stress-engineering strain curves of the CA-added and CA-free PHBV/PLGA (25:75)  
10 membrane at an initial strain rate of  $1 \times 10^{-3} \text{ s}^{-1}$ . At this strain rate, it is clear that adding 1%  
11 CA increased the strength with sacrificing from ductility and 5% CA increased the ductility  
12 with sacrificing from strength (Figure 4c). Therefore, CA should be added considering  
13 whether the strength or ductility is required in the application at this strain rate. Figure 4d  
14 shows the engineering stress-engineering strain curves of the CA-added and CA-free  
15 PHBV/PLGA (25:75) membrane at an initial strain rate of  $1 \times 10^{-4} \text{ s}^{-1}$ . At this strain rate,  
16 addition of 1% CA decreased the strength with enhancing the ductility, slightly but addition of  
17 5% CA increased both the strength and ductility of the membrane. Therefore, 5% CA added  
18 membrane can be used at this strain rate regardless of ductility or strength considerations.  
19 Even though, the effects of CA on the mechanical properties have never been investigated in  
20 the literature, the effects of fiber radius, decreased with CA addition (Figure 1, 2), were  
21 discussed by several authors and the detailed discussion was given in the paragraph after next.  
22  
23  
24  
25  
26  
27  
28  
29  
30  
31  
32  
33  
34  
35  
36  
37  
38  
39  
40  
41  
42  
43  
44  
45  
46  
47  
48  
49  
50  
51  
52  
53  
54  
55  
56  
57  
58  
59  
60



**Figure 4:** Engineering tensile stress-strain behavior of electrospun PHBV/PLGA (25:75) membranes with different *Centella Asiatica* concentrations in their chemical composition a)  $1 \times 10^{-1} \text{ s}^{-1}$ , b)  $1 \times 10^{-2} \text{ s}^{-1}$ , c)  $1 \times 10^{-3} \text{ s}^{-1}$ , d)  $1 \times 10^{-4} \text{ s}^{-1}$ .

Figure 5 a-d show the mechanical response sensitivity of PHBV/PCL membranes to the blend ratio. Figure 5a shows the engineering stress-strain curves at an initial strain rate of  $1 \times 10^{-1} \text{ s}^{-1}$ . Generally, increasing the PCL concentration in the chemical composition increased the strength without affecting the ductility considerably. However, PHBV/PCL (25:75) exhibited the best combination of strength and ductility among all membranes at this strain rate and it can be used in both high strength and ductility required applications. Figure 5b shows the mechanical response of the membranes at an initial strain rate of  $1 \times 10^{-2} \text{ s}^{-1}$ . Lowering the strain rate decreased the ductility of PHBV (100) and PHBV/PCL (75:25) membranes, however rest of the blends became stronger and more ductile. In particular, tensile strength

1  
2  
3 and ductility of PHBV/PCL (50:50) and PHBV/PCL (25:75) shifted up approximately 0.5  
4 MPa and 100%, respectively. At this strain rate, both the strength and ductility of the  
5 membranes were linearly proportional to the PCL concentration. Figure 5c shows mechanical  
6 response of the membranes at an initial strain rate of  $1 \times 10^{-3} \text{ s}^{-1}$  and previous linear  
7 relationship was also observed at this strain rate. Figure 5c shows mechanical response of the  
8 membranes at an initial strain rate of  $1 \times 10^{-4} \text{ s}^{-1}$ . At this strain rate, PHBV/PCL (25:75)  
9 exhibited the best combination of strength and ductility among all membranes like the fastest  
10 strain rate case. In addition, increasing PCL concentration up to 75% enhanced the strength  
11 and ductility of membranes but further increase in PCL concentration deteriorated the  
12 mechanical properties. PCL has been blended with different bio/polymers to obtain more  
13 advantageous nanofibrous scaffolds in the literature, and the results of the PCL blend  
14 membranes related to the improved mechanical properties given herein are consistent well  
15 with previous studies [38].  
16  
17  
18  
19  
20  
21  
22  
23  
24  
25  
26  
27  
28  
29  
30  
31  
32  
33  
34  
35  
36  
37  
38  
39  
40  
41  
42  
43  
44  
45  
46  
47  
48  
49  
50  
51  
52  
53  
54  
55  
56  
57  
58  
59  
60



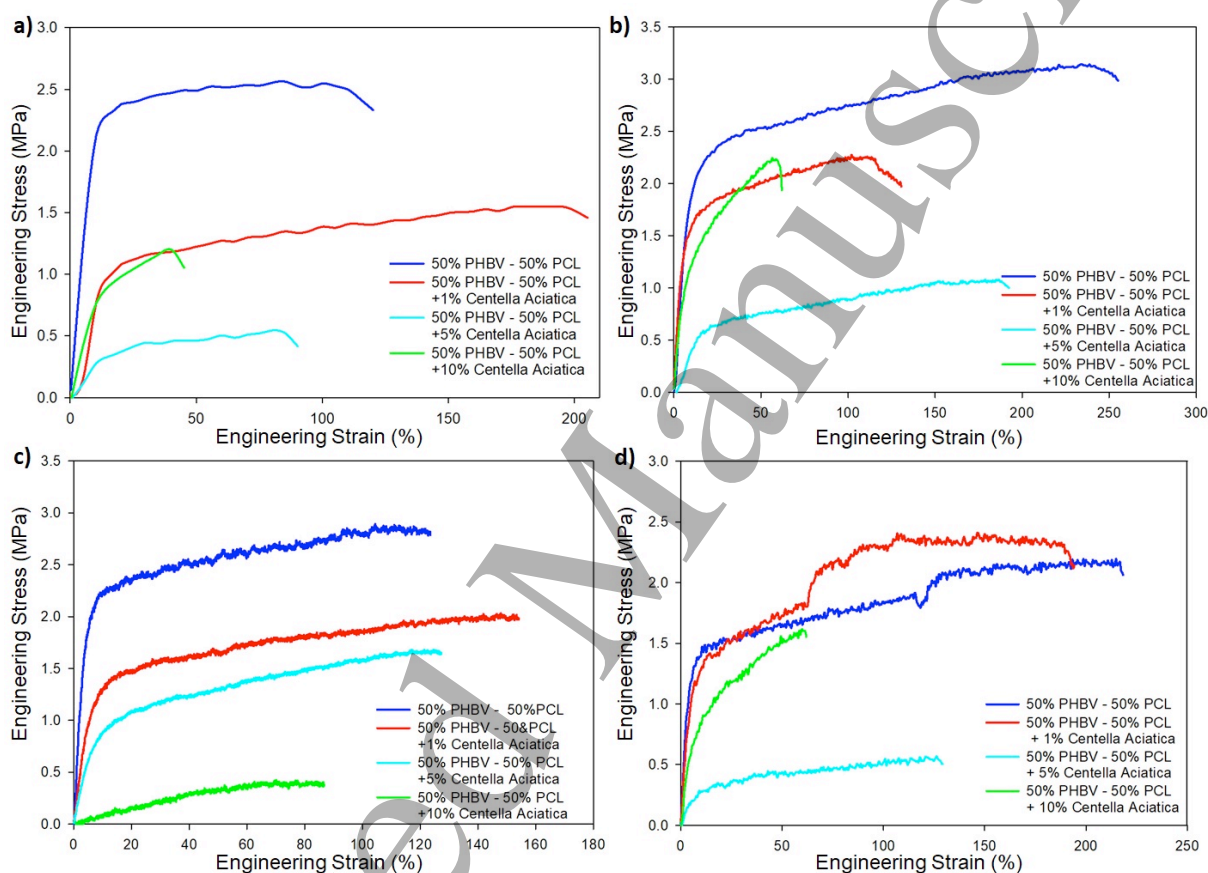
**Figure 5:** Engineering tensile stress-strain behavior of electrospun PHBV/PCL membranes in different blend ratios a)  $1 \times 10^{-1} \text{ s}^{-1}$ , b)  $1 \times 10^{-2} \text{ s}^{-1}$ , c)  $1 \times 10^{-3} \text{ s}^{-1}$ , d)  $1 \times 10^{-4} \text{ s}^{-1}$ .

Figure 6 a-d show the effects of CA on the mechanical response of electrospun PHBV/PCL (50:50) membrane at different strain rates. It was observed that adding CA into the chemical composition altered the mechanical properties of the PHBV/PCL (50:50) membrane and it generally degraded the strength at all strain rate range. However, there was no direct relationship between the mechanical properties and the amount of CA in the membrane. Figure 6a shows the engineering stress-engineering strain curves of the CA-added and CA-free PHBV/PCL (50:50) membrane at an initial strain rate of  $1 \times 10^{-1} \text{ s}^{-1}$ . At this strain rate, addition of very few amount of CA doubled the ductility from level to 208%. Increasing CA concentration from 1% to 5% decreased the strength and ductility, dramatically. On the other hand, further increase in CA concentration up to 10% recovered the strength but still

1  
2  
3 decreased the ductility. Figure 6b shows the engineering stress-engineering strain curves of  
4 the CA-added and CA-free PHBV/PCL (50:50) membrane at an initial strain rate of  $1 \times 10^{-2} \text{ s}^{-1}$   
5  
6  
7  
8  
9  
10  
11  
12  
13  
14  
15  
16  
17  
18  
19  
20  
21  
22  
23  
24  
25  
26  
27  
28  
29  
30  
31  
32  
33  
34  
35  
36  
37  
38  
39  
40  
41  
42  
43  
44  
45  
46  
47  
48  
49  
50  
51  
52  
53  
54  
55  
56  
57  
58  
59  
60

1. Lowering the strain rate by one order of magnitude increased the strength of all the membranes. The effects of CA on the strength of membrane at this strain rate is same with the previous case. However, adding CA always decreased the ductility when compared to CA-free membrane and 5% CA-added membrane showed the best ductility among all CA-added membranes. Figure 6c shows the engineering stress-engineering strain curves of the CA-added and CA-free PHBV/PCL (50:50) membrane at an initial strain rate of  $1 \times 10^{-3} \text{ s}^{-1}$ . The more CA concentration in the chemical concentration, the less strength and ductility values were observed at this strain rate. In addition, adding 1% CA enhanced the ductility like the first case with sacrificing strength. Therefore, 1% CA-added membrane can be used in the ductility required application areas over CA-free membrane, if the possible loadings do not create a stress more than 1.4 MPa and 1.8 MPa at the strain rates of  $1 \times 10^{-1} \text{ s}^{-1}$  and  $1 \times 10^{-3} \text{ s}^{-1}$ , respectively. Figure 6d shows the engineering stress-engineering strain curves of the CA-added and CA-free PHBV/PCL (50:50) membrane at an initial strain rate of  $1 \times 10^{-4} \text{ s}^{-1}$ . Addition of 1%CA to the chemical composition increased the tensile strength of a membrane from 2.0 MPa to 2.5 MPa. Improvement in the strength came with a slight deterioration in the ductility, from 220% to 190%. However, further increase in the CA concentration to 5% decreased the strength and ductility drastically but strength was recovered by increasing CA concentration to 10%, which caused more reduction in ductility. The relation between fiber radii, which was inversely proportional to the CA concentration, and the strength of polymers was investigated in the literature by several researchers [39–41]. Even though, the deterioration in the strength of PHBV/PCL (50:50) membrane with decreasing fiber radii by the addition of CA is in contradiction with previous results reported in the literature [41], the mechanical properties of bulk form of these kind of nanofibrous materials are highly

dependent to other structural parameters such as linearity of the fibers [42], membrane porosity [42,43], fiber alignment such as bead and defects, cross linkages [42–44], number of fiber-fiber interactions [40,44]. Furthermore, the supramolecular structure also matters to define mechanical responses of bulk materials as discussed by Arinstein et al. [45]. That is why, there is no direct relationship between the strength of a membrane with the fiber radii.



**Figure 6:** Engineering tensile stress-strain behavior of electrospun PHBV/PCL (50:50) membranes with different Centella Asiatica concentrations in their chemical composition a)  $1 \times 10^{-1} \text{ s}^{-1}$ , b)  $1 \times 10^{-2} \text{ s}^{-1}$ , c)  $1 \times 10^{-3} \text{ s}^{-1}$ , d)  $1 \times 10^{-4} \text{ s}^{-1}$ .

Figure 7 a-d show the mechanical properties of PLGA vs. PCL membranes and compare their response when they blend with PHBV. Figure 7a shows mechanical response of the membranes at an initial strain rate of  $1 \times 10^{-1} \text{ s}^{-1}$ . At this strain rate, it was observed that, 100% PLGA exhibited more strength and ductility values than 100% PCL membrane. Moreover, at

1  
2  
3 the same PHBV concentration of 50%, 50% PLGA increased the strength of a membrane  
4 much more than 50% PCL. On the other hand, at the same PHBV concentration of 25%, 75%  
5  
6 PCL gave better performance than 75% PLGA in terms of both ductility and strength. Figure  
7  
8 7b shows mechanical response of the membranes at an initial strain rate of  $1 \times 10^{-2} \text{ s}^{-1}$ . 100%  
9  
10 PCL membrane showed extraordinary ductility without sacrificing from its strength by  
11  
12 lowering the strain rate by one order of magnitude and it was stronger and more ductile than  
13  
14 PLGA membrane. In addition, when the PHBV concentration was 50% in the blend, 50%  
15  
16 PLGA showed more strength and 50% PCL showed more ductility. That means, the  
17  
18 PHBV/PLGA (50:50) or PHBV/PCL (50:50) membranes can be used at the strain rate of  $1 \times$   
19  
20  $10^{-2} \text{ s}^{-1}$  if the application is stress or ductility required, respectively. Figure 7c shows  
21  
22 mechanical response of the membranes at an initial strain rate of  $1 \times 10^{-3} \text{ s}^{-1}$ . Likewise, to the  
23  
24 previous case, 100% PCL membrane was more ductile and stronger than 100% PLGA  
25  
26 membrane. In addition, compared to the 50% PLGA containing membranes, 50% PCL had  
27  
28 more positive effects on the mechanical properties of membranes that contain 50% PHBV.  
29  
30 Similarly, at the same PHBV concentration of 25%, 75% PCL resulted better mechanical  
31  
32 properties than 75% PLGA membrane. Specifically, the ductility of the PHBV/PCL (25:75)  
33  
34 membrane was 8 times greater than the ductility of the PHBV/PLGA (25:75) membrane and  
35  
36 the strength of a PHBV/PCL (25:75) membrane was almost 1.5 times greater than the strength  
37  
38 of the PHBV/PLGA (25:75) membrane. Figure 7d shows mechanical response of the  
39  
40 membranes at an initial strain rate of  $1 \times 10^{-4} \text{ s}^{-1}$ . Specifically, 100% PCL membrane had  
41  
42 almost 3 times more stress values than 100% PLGA membrane with a same ductility at the  
43  
44 quasi-static strain rate. In addition, even though PHBV/PLGA (50:50) blend was stronger  
45  
46 than PHBV/PCL (50:50) blend up to 80% engineering strain, PHBV/PCL (50:50) membrane  
47  
48 is more ductile and it can withstand more loads via plastic deformation. Moreover, at the same  
49  
50  
51  
52  
53  
54  
55  
56  
57  
58  
59  
60

PHBV concentration of 25%, 75% PCL resulted much more ductility and strength than 75% PLGA.

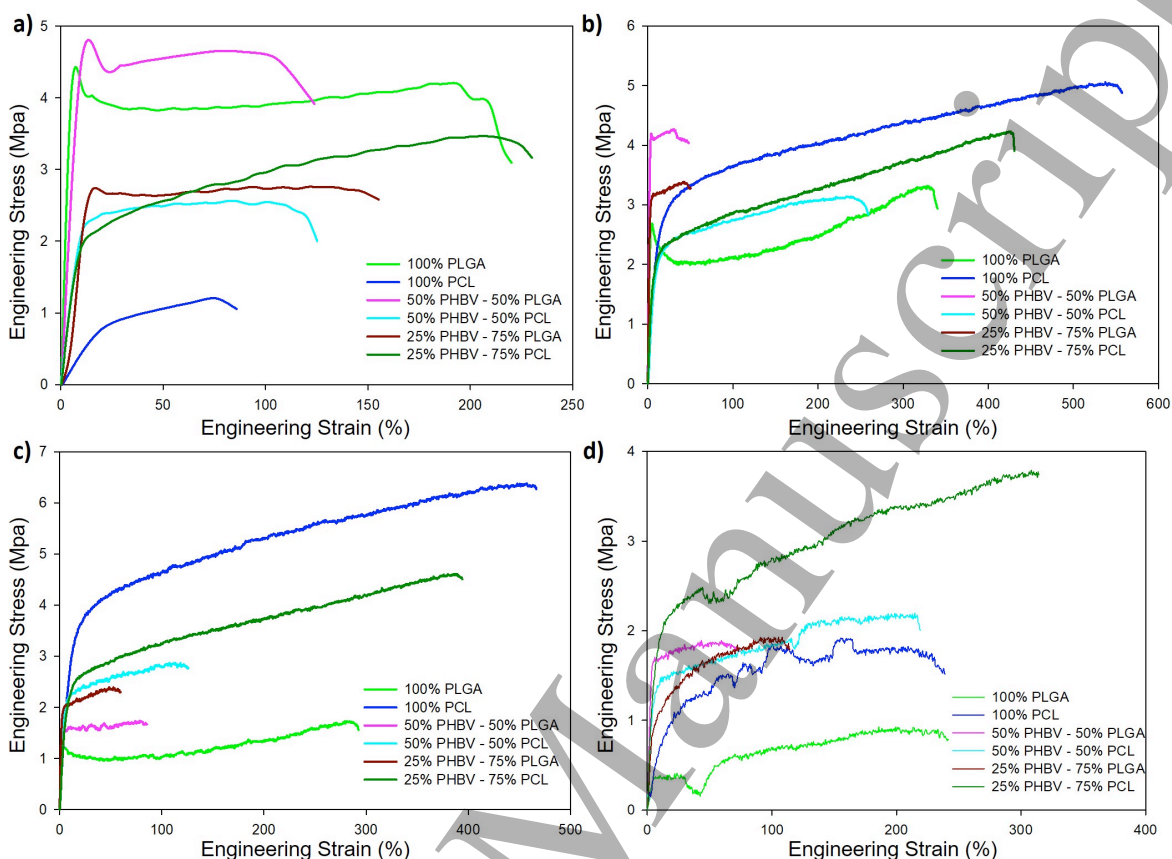


**Figure 7:** Engineering tensile stress-strain behavior of electrospun PLGA, PCL, PHBV/PLGA and PHBV/PCL membranes with different blend ratios a)  $1 \times 10^{-1} \text{ s}^{-1}$ , b)  $1 \times 10^{-2} \text{ s}^{-1}$ , c)  $1 \times 10^{-3} \text{ s}^{-1}$ , d)  $1 \times 10^{-4} \text{ s}^{-1}$ .

The graphical representation of the measured mechanical properties of the PHBV/PLGA and PHBV/PCL membranes at the highest and lowest strain rates is given in Figure 8. The Gaussian method was used to draw continuous strain rate curves. Red curves represent the mechanical responses at the initial strain rate of  $1 \times 10^{-1} \text{ s}^{-1}$  and the green curves represent the mechanical responses at the initial strain rate of  $1 \times 10^{-4} \text{ s}^{-1}$ . It is clear that PHBV/PLGA membrane showed positive strain rate sensitivity after 20% PLGA composition in the chemical composition (Figure 8a). Specifically, the tensile strength was linearly proportional

1  
2  
3 to the strain rate. This behavior is commonly observed in most of the materials since as the  
4 material is deformed at a faster rate, the density of hardening/plastic deformation mechanisms  
5 and their interactions increases, and leads to an increased level of stress at the same strain  
6 levels [37,46]. It has been reported that semi-crystalline polymers, such as PCL, PHBV,  
7 PLGA, contain many layers emanating from screw dislocations and movement of these  
8 dislocations causes the plastic deformation [47,48]. To a large extent, once the material is  
9 deformed at faster rate, much more dislocation activated and their density and mobility  
10 increases rapidly and result in greater stress values at the same strain. In addition, the tensile  
11 strength of a PHBV/PLGA blend increased with increasing PLGA composition up to 50% but  
12 further increase in the PLGA composition up to 80% deteriorated the tensile strength of a  
13 PHBV/PLGA membrane at both strain rates. Similarly, Young's modulus of PHBV/PLGA  
14 membrane changed with PLGA composition and the corresponding change was shown in  
15 Figure 8b. Specifically, at the fastest strain rate, the greatest tensile strength and Young's  
16 modulus of a PHBV/PLGA membrane were obtained at 90% PLGA and 100% PLGA,  
17 respectively and at the quasi-static strain rate, the greatest tensile strength and Young's  
18 modulus were determined at 50% PLGA (Figure 8a, Figure 8b). Figure 8c and 8d shows the  
19 dependence of tensile strength and Young's modulus on the PCL composition in the  
20 PHBV/PCL membranes at the aforementioned strain rates. In particular, negative strain rate  
21 sensitivity was observed until the 50% PCL composition and further increase in the PCL  
22 composition triggered positive strain rate sensitivity (Figure 8c). Specifically, 20% PCL and  
23 80% PCL promoted the greatest stress levels in PHBV/PCL membrane at the slowest strain  
24 rate and fastest strain rate, respectively (Figure 8c). Furthermore, Young's modulus of a  
25 PHBV/PCL membrane was generally linear proportional to the PCL composition in the  
26 membrane until 50% PCL but further increase in PCL composition caused to decrease in  
27 young's modulus at both the quasi static strain rate and the fastest strain rate (Figure 8d). The  
28  
29  
30  
31  
32  
33  
34  
35  
36  
37  
38  
39  
40  
41  
42  
43  
44  
45  
46  
47  
48  
49  
50  
51  
52  
53  
54  
55  
56  
57  
58  
59  
60

numerical values of the mechanical properties of the selected membranes at the initial strain rate of  $1 \times 10^{-1} \text{ s}^{-1}$  were listed in Table 1. The trend of changes in the tensile strength and Young's modulus with blend ratio corresponds well with previous studies [49].

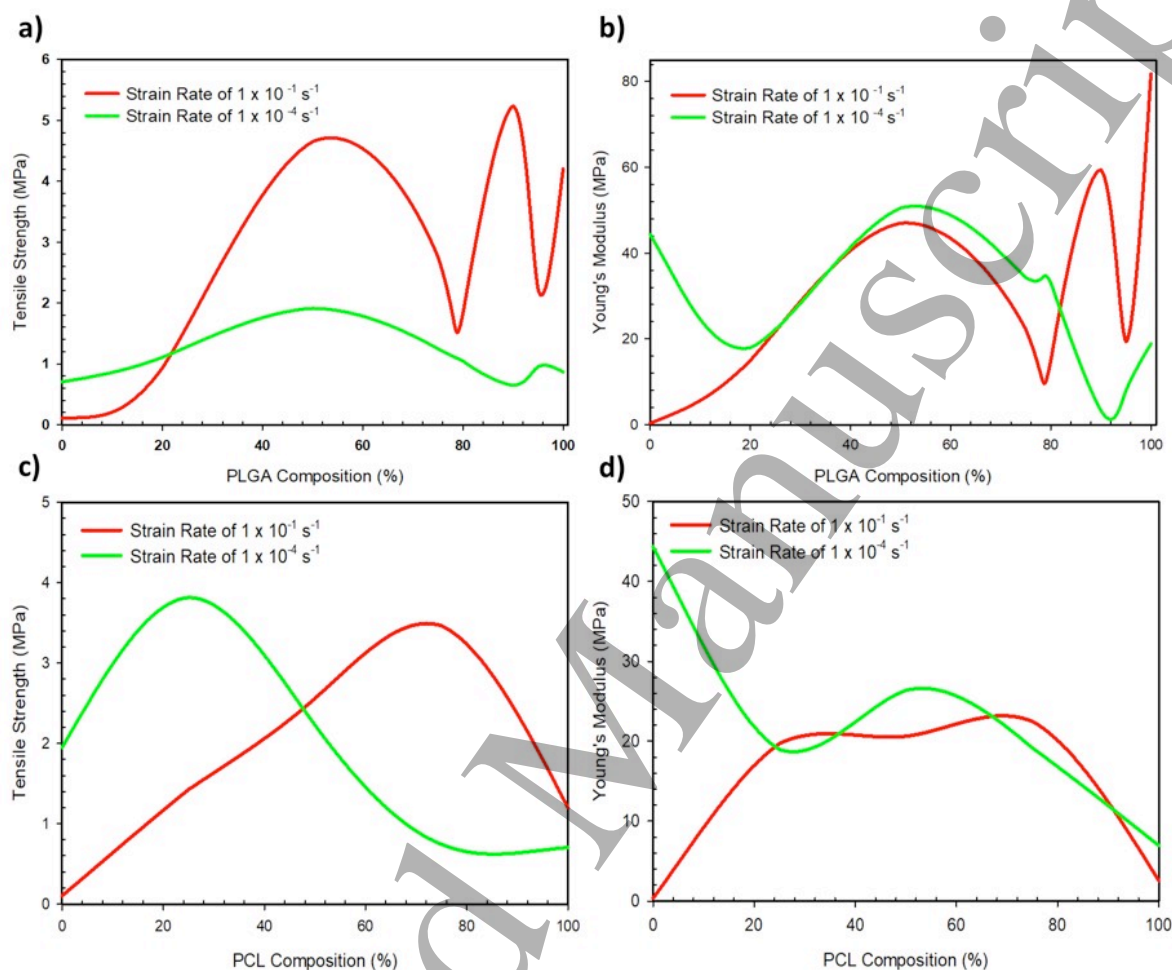


**Figure 8:** Graphical representation of the mechanical properties of the PHBV/PLGA (a, b) and PHBV/PCL (c, d) membranes a) PLGA Composition vs Tensile Strength, b) PLGA Composition vs Young's Modulus, c) PCL Composition vs Tensile Strength, d) PCL Composition vs Young's Modulus.

Table 1: Tensile test results of selected membranes at the initial strain rate of  $1 \times 10^{-1} \text{ s}^{-1}$ .

Sample	Tensile Strength (Mpa)	Elongation (%)	Young's Modulus (Mpa)
--------	------------------------	----------------	-----------------------

<b>PHBV (100%, w/w)</b>	0.1	108.32	0.34
<b>PLGA (100%, w/w)</b>	4.2	224.66	81.83
<b>PCL (100, % w/w)</b>	1.2	80	2.56
<b>PHBV/PLGA (50:50%, w/w)</b>	4.65	125.65	47
<b>PHBV/PLGA (25:75%, w/w)</b>	2.76	166.09	22.22
<b>PHBV/PLGA (25:75%, w/w)</b>	2.06	150	10
<b>+ 1% CA</b>			
<b>PHBV/PLGA (25:75%, w/w)</b>	5.81	90	40
<b>+ 5% CA</b>			
<b>PHBV/PLGA (20:80%, w/w)</b>	1.83	237.93	14.94
<b>PHBV/PLGA (10:90%, w/w)</b>	5.24	237.94	59.42
<b>PHBV/PCL (50:50%, w/w)</b>	2.56	115	20.63
<b>PHBV/PCL (50:50%, w/w)+</b>	1.55	210	7.47
<b>1% CA</b>			
<b>PHBV/PCL (50:50%, w/w) +</b>	0.54	85	2.69
<b>5% CA</b>			
<b>PHBV/PCL (50:50%, w/w) +</b>	1.2	43	7.44
<b>10% CA</b>			
<b>PHBV/PCL (25:75%, w/w)</b>	3.47	239.51	22.5

#### 4. Conclusions

In this study, the effects of chemical composition, strain rate, and a traditional medicinal plant, *Centella Asiatica* (CA), on the mechanical responses of the PHBV/PCL and PHBV/PLGA blend electrospun nonwoven mats were investigated by tensile testing at room temperature. In particular, the best and worst combinations of PHBV/PLGA, PHBV/PCL blend ratios for both stress and ductility required applications were specified at each strain rate. It was observed that the addition of PLGA improved the strength and ductility of the PHBV, significantly. Specifically, after 75% PLGA concentration in the blend ductility increases, rapidly. Also, the effects of CA on the fiber diameter were discussed in the current study and it was concluded that CA addition generally degraded the strength of PHBV/PCL (50:50) membrane at all strain rate range. In addition, it was observed that the stress required for yield initiation is greater than the stress required for yield propagation. Overall, this study presented herein opens a new venue for selection and usage of the aforementioned electrospun mats in terms of mechanical behavior under a wide range of strain rates.

#### Acknowledgments

B. Bal acknowledges the financial support by the AGU-BAP under grant number FAB-2017-77 and I. A. Isoglu acknowledges the financial support by the AGU-BAP under grant number FOA-2016-76.

#### References

- [1] T.G. Sahana, P.D. Rekha, Biopolymers: Applications in wound healing and skin tissue engineering, *Mol. Biol. Rep.* **45** (2018) 2857–2867. doi:10.1007/s11033-018-4296-3.
- [2] M. Norouzi, S.M. Boroujeni, N. Omidvarkordshouli, M. Soleimani, Advances in Skin Regeneration: Application of Electrospun Scaffolds, *Adv. Healthc. Mater.* **4** (2015) 1114–1133. doi:10.1002/adhm.201500001.
- [3] P. Basu, U. Narendra Kumar, I. Manjubala, Wound healing materials - A perspective for skin tissue engineering, *Curr. Sci.* **112** (2017) 2392–2404. doi:10.18520/cs/v112/i12/2392-2404.

- 1  
2  
3 [4] M.R. MacEwan, S. MacEwan, T.R. Kovacs, J. Batts, What Makes the Optimal Wound Healing  
4 Material? A Review of Current Science and Introduction of a Synthetic Nanofabricated Wound  
5 Care Scaffold, *Cureus*. **9** (2017). doi:10.7759/cureus.1736.  
6  
7 [5] S.P. Miguel, D.R. Figueira, D. Simões, M.P. Ribeiro, P. Coutinho, P. Ferreira, I.J. Correia,  
8 Electrospun polymeric nanofibres as wound dressings: A review, *Colloids Surfaces B*  
9 *Biointerfaces*. **169** (2018) 60–71. doi:10.1016/j.colsurfb.2018.05.011.  
10  
11 [6] A. Chanda, J. Adhikari, A. Ghosh, S.R. Chowdhury, S. Thomas, P. Datta, P. Saha, Electrospun  
12 chitosan/polycaprolactone-hyaluronic acid bilayered scaffold for potential wound healing  
13 applications, *Int. J. Biol. Macromol.* **116** (2018) 774–785. doi:10.1016/j.ijbiomac.2018.05.099.  
14  
15 [7] M. Ignatova, I. Rashkov, N. Manolova, Drug-loaded electrospun materials in wound-dressing  
16 applications and in local cancer treatment, *Expert Opin. Drug Deliv.* **10** (2013) 469–483.  
17 doi:10.1517/17425247.2013.758103.  
18  
19 [8] Y.F. Goh, I. Shakir, R. Hussain, Electrospun fibers for tissue engineering, drug delivery, and  
20 wound dressing, *J. Mater. Sci.* **48** (2013) 3027–3054. doi:10.1007/s10853-013-7145-8.  
21  
22 [9] M. Liu, X.P. Duan, Y.M. Li, D.P. Yang, Y.Z. Long, Electrospun nanofibers for wound healing,  
23 *Mater. Sci. Eng. C*. **76** (2017) 1413–1423. doi:10.1016/j.msec.2017.03.034.  
24  
25 [10] A. Cipitria, A. Skelton, T.R. Dargaville, P.D. Dalton, D.W. Hutmacher, Design, fabrication and  
26 characterization of PCL electrospun scaffolds - A review, *J. Mater. Chem.* **21** (2011) 9419–  
27 9453. doi:10.1039/c0jm04502k.  
28  
29 [11] S. Chen, B. Liu, M.A. Carlson, A.F. Gombart, D.A. Reilly, J. Xie, Recent advances in electrospun  
30 nanofibers for wound healing., *Nanomedicine (Lond)*. **12** (2017) 1335–1352.  
31 doi:10.2217/nnm-2017-0017.  
32  
33 [12] J.R. Dias, P.L. Granja, P.J. Bártolo, Advances in electrospun skin substitutes, *Prog. Mater. Sci.*  
34 **84** (2016) 314–334. doi:10.1016/j.pmatsci.2016.09.006.  
35  
36 [13] D. Zhang, X. Wu, J. Chen, K. Lin, The development of collagen based composite scaffolds for  
37 bone regeneration, *Bioact. Mater.* **3** (2018) 129–138. doi:10.1016/j.bioactmat.2017.08.004.  
38  
39 [14] E. Malikmammadov, T.E. Tanir, A. Kiziltay, V. Hasirci, N. Hasirci, PCL and PCL-based materials  
40 in biomedical applications, *J. Biomater. Sci. Polym. Ed.* **29** (2018) 863–893.  
41 doi:10.1080/09205063.2017.1394711.  
42  
43 [15] N. Tra Thanh, M. Ho Hieu, N. Tran Minh Phuong, T. Do Bui Thuan, H. Nguyen Thi Thu, V.P.  
44 Thai, T. Do Minh, H. Nguyen Dai, V.T. Vo, H. Nguyen Thi, Optimization and characterization of  
45 electrospun polycaprolactone coated with gelatin-silver nanoparticles for wound healing  
46 application, *Mater. Sci. Eng. C*. **91** (2018) 318–329. doi:10.1016/j.msec.2018.05.039.  
47  
48 [16] A. Ehterami, M. Salehi, S. Farzamfar, A. Vaez, H. Samadian, H. Sahrapeyma, M. Mirzaii, S.  
49 Ghorbani, A. Goodarzi, In vitro and in vivo study of PCL/COLL wound dressing loaded with  
50 insulin-chitosan nanoparticles on cutaneous wound healing in rats model, *Int. J. Biol.*  
51 *Macromol.* **117** (2018) 601–609. doi:10.1016/j.ijbiomac.2018.05.184.  
52  
53 [17] C. Del Gaudio, E. Ercolani, F. Nanni, A. Bianco, Assessment of poly(e{open}-  
54 caprolactone)/poly(3-hydroxybutyrate-co-3-hydroxyvalerate) blends processed by solvent  
55 casting and electrospinning, *Mater. Sci. Eng. A*. **528** (2011) 1764–1772.  
56 doi:10.1016/j.msea.2010.11.012.  
57  
58  
59  
60

- 1  
2  
3 [18] R. Jain, A. Tiwari, Role of polyhydroxyalkanoates in cancer and other drug delivery systems, *J. Cancer Res. Ter.* **11** (2015) 494–495. doi:10.4103/0973-1482.140784.
- 4  
5  
6 [19] G.Q. Chen, Q. Wu, The application of polyhydroxyalkanoates as tissue engineering materials, *Biomaterials.* **26** (2005) 6565–6578. doi:10.1016/j.biomaterials.2005.04.036.
- 7  
8  
9 [20] R. Shi, H. Geng, M. Gong, J. Ye, C. Wu, X. Hu, L. Zhang, Long-acting and broad-spectrum  
10 antimicrobial electrospun poly ( $\epsilon$ -caprolactone)/gelatin micro/nanofibers for wound dressing,  
11 *J. Colloid Interface Sci.* **509** (2018) 275–284. doi:10.1016/j.jcis.2017.08.092.
- 12  
13 [21] J. Liao, Y. Jia, B. Wang, K. Shi, Z. Qian, Injectable Hybrid Poly( $\epsilon$ -caprolactone)- b -poly(ethylene  
14 glycol)- b -poly( $\epsilon$ -caprolactone) Porous Microspheres/Alginate Hydrogel Cross-linked by  
15 Calcium Gluconate Crystals Deposited in the Pores of Microspheres Improved Skin Wound  
16 Healing, *ACS Biomater. Sci. Eng.* **4** (2018) 1029–1036. doi:10.1021/acsbomaterials.7b00860.
- 17  
18 [22] F.A. Paskiabi, S. Bonakdar, M.A. Shokrgozar, M. Imani, Z. Jahanshiri, M. Shams-Ghahfarokhi,  
19 M. Razzaghi-Abyaneh, Terbinafine-loaded wound dressing for chronic superficial fungal  
20 infections, *Mater. Sci. Eng. C.* **73** (2017) 130–136. doi:10.1016/j.msec.2016.12.078.
- 21  
22 [23] S.Y.H. Abdalkarim, H.Y. Yu, D. Wang, J. Yao, Electrospun poly(3-hydroxybutyrate-co-3-hydroxy-  
23 valerate)/cellulose reinforced nanofibrous membranes with ZnO nanocrystals for antibacterial  
24 wound dressings, *Cellulose.* **24** (2017) 2925–2938. doi:10.1007/s10570-017-1303-0.
- 25  
26 [24] C. Lei, H. Zhu, J. Li, J. Li, X. Feng, J. Chen, PHBV/silk fibroin nanofibrous scaffolds for repairing  
27 of skin tissue, *Polym. Eng. Sci.* **55** (2015) 907–916. doi:10.1002/pen.
- 28  
29 [25] J. Varshosaz, A. Jahanian, M. Maktoobian, Montelukast incorporated poly(methyl vinyl ether-  
30 co-maleic acid)/poly(lactic-co-glycolic acid) electrospun nanofibers for wound dressing, *Fibers*  
31 *Polym.* **18** (2017) 2125–2134. doi:10.1007/s12221-017-7438-7.
- 32  
33 [26] X. Liu, L.H. Nielsen, S.N. Kłodzińska, H.M. Nielsen, H. Qu, L.P. Christensen, J. Rantanen, M.  
34 Yang, Ciprofloxacin-loaded sodium alginate/poly (lactic-co-glycolic acid) electrospun fibrous  
35 mats for wound healing, *Eur. J. Pharm. Biopharm.* **123** (2018) 42–49.  
36 doi:10.1016/j.ejpb.2017.11.004.
- 37  
38 [27] S. Tohidi, A. Ghaee, J. Barzin, Preparation and characterization of poly(lactic-co-glycolic  
39 acid)/chitosan electrospun membrane containing amoxicillin-loaded halloysite nanoclay,  
40 *Polym. Adv. Technol.* **27** (2016) 1020–1028. doi:10.1002/pat.3764.
- 41  
42 [28] D. Daranarong, R. T. H. Chan, N. S. Wanandy, R. Molloy, W. Punyodom, L. J. R. Foster,  
43 Electrospun Polyhydroxybutyrate and Poly(L-Lactide-Co- $\epsilon$ -Caprolactone) Composites as  
44 Nanofibrous Scaffolds, *Biomed Res. Int.* **2014** (2014) . doi:10.1155/2014/741408 1-12.
- 45  
46 [29] Y. Ding, W. Li, T. Müller, D. W. Schubert, A.R. Boccaccini, Q. Yao, J. A. Roether, Electrospun  
47 Polyhydroxybutyrate/Poly( $\epsilon$ -Caprolactone)/58S Sol-Gel Bioactive Glass Hybrid Scaffolds with  
48 Highly Improved Osteogenic Potential for Bone Tissue Engineering, *ACS Appl. Mater.*  
49 *Interfaces.* **8** (2016) 17098–17108. doi: 10.1021/acsaami.6b03997.
- 50  
51 [30] F. Ublekov, D. Budurova, M. Staneva, M. Natova, H. Penchev, Self-Supporting Electrospun PHB  
52 and PHBV/Organoclay Nanocomposite Fibrous Scaffolds, *Mater. Lett.* **218** (2018) 353–356.  
53 doi:10.1016/j.matlet.2018.02.056.
- 54  
55 [31] F. Croisier, A.S. Duwez, C. Jérôme, A.F. Léonard, K.O. Van Der Werf, P.J. Dijkstra, M.L. Bennink,  
56 Mechanical testing of electrospun PCL fibers, *Acta Biomater.* **8** (2012) 218–224.  
57 doi:10.1016/j.actbio.2011.08.015.
- 58  
59  
60

- 1  
2  
3 [32] A. Baji, Y.W. Mai, S.C. Wong, M. Abtahi, P. Chen, Electrospinning of polymer nanofibers:  
4 Effects on oriented morphology, structures and tensile properties, *Compos. Sci. Technol.* **70**  
5 (2010) 703–718. doi:10.1016/j.compscitech.2010.01.010.  
6
- 7 [33] S. Manotham, K. Pengpat, S. Eitssayeam, G. Rujijanagul, D.R. Sweatman, T. Tunkasiri,  
8 Fabrication of Polycaprolactone/Centella asiatica Extract Biopolymer Nanofiber by  
9 Electrospinning, *Appl. Mech. Mater.* **804** (2015) 151–154.  
10 doi:10.4028/www.scientific.net/AMM.804.151.  
11
- 12 [34] P. Sikareepaisan, A. Suksamrarn, P. Supaphol, Electrospun gelatin fiber mats containing a  
13 herbal - Centella asiatica - Extract and release characteristic of asiaticoside, *Nanotechnology.*  
14 **19** (2008). doi:10.1088/0957-4484/19/01/015102.  
15
- 16 [35] R.A. Franco, T.H. Nguyen, B.T. Lee, Preparation and characterization of electrospun PCL/PLGA  
17 membranes and chitosan/gelatin hydrogels for skin bioengineering applications, *J. Mater. Sci.*  
18 *Mater. Med.* **22** (2011) 2207–2218. doi:10.1007/s10856-011-4402-8.  
19
- 20 [36] L. Brown, I.M. Ward, Load Drop at the Upper Yield Point of a Polymer, *J. Polym. Sci. Part A-2.* **6**  
21 (1968) 607–620. doi:10.1002/pol.1968.160060314.  
22
- 23 [37] B. Bal, B. Gumus, D. Canadinc, Incorporation of Dynamic Strain Aging into a Viscoplastic Self-  
24 Consistent Model for Predicting the Negative Strain Rate Sensitivity of Hadfield Steel, *J. Eng.*  
25 *Mater. Technol. Trans. ASME.* **138** (2016) 1–8. doi:10.1115/1.4033072.  
26
- 27 [38] D. Gupta, J. Venugopal, M.P. Prabhakaran, V.R.G. Dev, S. Low, A.T. Choon, S. Ramakrishna,  
28 Aligned and random nanofibrous substrate for the in vitro culture of Schwann cells for neural  
29 tissue engineering, *Acta Biomater.* **5** (2009) 2560–2569. doi:10.1016/j.actbio.2009.01.039.  
30
- 31 [39] T. Stylianopoulos, C.A. Bashur, A.S. Goldstein, S.A. Guelcher, V.H. Barocas, Computational  
32 predictions of the tensile properties of electrospun fibre meshes: Effect of fibre diameter and  
33 fibre orientation, *J. Mech. Behav. Biomed. Mater.* **1** (2008) 326–335.  
34 doi:10.1016/j.jmbbm.2008.01.003.  
35
- 36 [40] X. Wei, Z. Xia, S.C. Wong, A. Baji, Modelling of mechanical properties of electrospun nanofibre  
37 network, *Int. J. Exp. Comput. Biomech.* **1** (2009) 45. doi:10.1504/IJECB.2009.022858.  
38
- 39 [41] S.C. Wong, A. Baji, S. Leng, Effect of fiber diameter on tensile properties of electrospun poly( $\epsilon$ -  
40 caprolactone), *Polymer (Guildf).* **49** (2008) 4713–4722. doi:10.1016/j.polymer.2008.08.022.  
41
- 42 [42] C.L. Pai, M.C. Boyce, G.C. Rutledge, On the importance of fiber curvature to the elastic moduli  
43 of electrospun nonwoven fiber meshes, *Polymer (Guildf).* (2011).  
44 doi:10.1016/j.polymer.2011.10.055.  
45
- 46 [43] T. Stylianopoulos, M. Kokonou, S. Michael, A. Tryfonos, C. Rebholz, A.D. Odysseos, C.  
47 Doumanidis, Tensile mechanical properties and hydraulic permeabilities of electrospun  
48 cellulose acetate fiber meshes, *J. Biomed. Mater. Res. Part B Appl. Biomater.* **100B** (2012)  
49 2222–2230. doi:10.1002/jbm.b.32791.  
50
- 51 [44] M.S. Rizvi, P. Kumar, D.S. Katti, A. Pal, Mathematical model of mechanical behavior of  
52 micro/nanofibrous materials designed for extracellular matrix substitutes, *Acta Biomater.* **8**  
53 (2012) 4111–4122. doi:10.1016/j.actbio.2012.07.025.  
54
- 55 [45] A. Arinstein, M. Burman, O. Gendelman, E. Zussman, Effect of supramolecular structure on  
56 polymer nanofibre elasticity, *Nat. Nanotechnol.* **2** (2007) 59–62. doi:10.1038/nnano.2006.172.  
57  
58  
59  
60

- 1  
2  
3 [46] D. Canadinc, C. Efstathiou, H. Sehitoglu, On the negative strain rate sensitivity of Hadfield  
4 steel, *Scr. Mater.* **59** (2008) 1103–1106. doi:10.1016/j.scriptamat.2008.07.027.  
5  
6 [47] E. Nunez, CRYSTALLISATION OF STAR POLYESTERS WITH POLY( $\epsilon$ -CAPROLACTONE) ARMS -  
7 Approaching the Problem of Early Stages in Polymer Crystallisation, 2004.  
8  
9 [48] F. Spieckermann, G. Polt, H. Wilhelm, M. Kerber, E. Schafner, M.J. Zehetbauer, The role of  
10 dislocations for the plastic deformation of semicrystalline polymers as investigated by  
11 multireflection X-ray line profile analysis, *J. Appl. Polym. Sci.* **125** (2012) 4150–4154.  
12 doi:10.1002/app.36570.  
13  
14 [49] T.O.F. Contents, Relationships between mechanical properties and drug release from  
15 electrospun fibers of PCL and PLGA blends, *J. Mech. Behav. Biomed. Mater.* **65** (2017) 724–  
16 733. doi:10.1109/ICHQP.2012.6381178.  
17  
18  
19  
20  
21  
22  
23  
24  
25  
26  
27  
28  
29  
30  
31  
32  
33  
34  
35  
36  
37  
38  
39  
40  
41  
42  
43  
44  
45  
46  
47  
48  
49  
50  
51  
52  
53  
54  
55  
56  
57  
58  
59  
60